

Shock Structure and Acoustic Waves in a Supersonic Jet

Catalina Stern Forgach and José Manuel Alvarado Reyes

Abstract Even though supersonic flows have been studied for a long time, many questions remain unanswered about their behavior. The understanding of jet noise goes in parallel with the understanding of jet turbulence. It has been speculated that different kinds of vortex interactions in the near field, can produce sound. Also, that the interaction between the flow and the shock structure produces noise. It is now known that noise, in supersonic and subsonic jets, is made up of two basic components; one from the large turbulence structures and instability waves, and the other from the fine-scale turbulence. Measurements inside a supersonic jet are difficult. Hot wires are easily broken and homogeneous seeding for Laser Doppler and Particle Image Velocimetries is complicated. We have developed a non-intrusive technique that uses the heterodyne detection of Rayleigh scattering. The laser light scattered elastically by the molecules of the flow at a particular angle, has information about density fluctuations of a particular size. It can be shown that the signal that comes out of a quadratic photo detector is proportional to the spatial Fourier transform as a function of time, of the density fluctuations for a wave vector given by the scattering angle. The spectral analysis of the data has allowed us to identify fluctuations of different origins; entropic and acoustic. We have taken data at many points inside and outside the flow. The technique is sensitive to the wave vector so we can study fluctuations that propagate in different directions. Fluctuations in the direction of the flow are shifted in frequency with respect to fluctuations perpendicular to the flow at the same location. The frequency shift allows us to measure the local speed of the flow. Outside the flow, only acoustic fluctuations are detected. We have been able to determine the far field acoustic radiation pattern for a given wave vector. Inside the jet, the analysis is much more complicated because the acoustic and the

C. S. Forgach (✉) · J. M. A. Reyes
Departamento de Física, Facultad de Ciencias, Universidad Nacional Autónoma de México,
UNAM, Circuito Exterior S/N, Ciudad Universitaria, CO 04510, México, D. F., Mexico
e-mail: catalinastern@gmail.com

J. M. A. Reyes
e-mail: mar_ney2003@yahoo.com.mx

entropic peaks overlap when we use simple Fourier transforms. However, with the use of parametric periodgrams we have been able to identify each type of fluctuation. Moreover, we found a third peak at a much lower frequency that appears and disappears as we move along the centerline of the jet. This peak appears also in other positions outside the centerline. We have used Rayleigh scattering and Schlieren to visualize the shock structure. We can then associate each spectrum with a position in the jet relative to the shock structure. The slow peak appears always at a shock, probably due to the interaction between the flow and the shock structure. We are now working on the visualization of the flow, and hope that the combination of all the techniques will give us further insight into the global behavior of the flow, especially in the interfaces between the flow and the shocks and between the mixing layer and the stationary fluid.

1 Introduction

Supersonic noise is of great importance in several industrial applications (Nichols et al. 2011). The objective of this work is to understand the production and propagation of acoustic waves in a supersonic jet. On one hand, there are several hypotheses about acoustic production in supersonic jets, related to vortex interactions in the mixing layer, the interaction between the flow and the shock structure, and to small scale turbulence. Each kind of aerodynamic events produces waves of different frequency (Bodonyy and Lele 2006). The traditional methods to study these flows are intrusive: hot wire anemometry, laser Doppler, or particle image velocimetries and sometimes involve complicated correlations of signals from three dimensional arrangements of microphones in the far acoustic field outside the flow with flow measurements in the near field. We hope to develop simpler methods to relate the acoustic field to aerodynamic events in the flow.

In the late seventies, in the *École Polytechnique* in France, a non-intrusive optical technique was developed to detect density fluctuations inside and outside of the flow (Stern and Grésillon 1983). This technique takes advantage of the heterodyne detection of laser light elastically scattered by the molecules of a transparent gas in motion (Rayleigh scattering). It can also be used to measure the mean velocity in the scattering volume. In the Hydrodynamic and Turbulence Laboratory in the Physics Department of the School of Science in UNAM, the technique has been complemented with signal processing methods that increase the resolution in frequency space and with different forms of visualization of the shock structure (Aguilar 2003).

The acoustic emission pattern for some frequencies has been measured with the technique mentioned. Also, with the help of visualizations, it has been possible to relate measurements of density fluctuations with the shock structure.

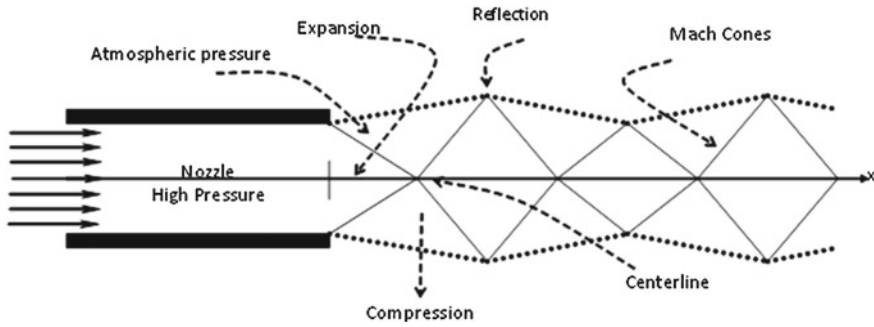


Fig. 1 The discontinuity at the end of the nozzle creates a perturbation that gives rise to a stationary shock pattern, when the flow is supersonic

2 Theoretical Background

In this section, some relevant concepts of supersonic flows will be reviewed first and then, some concepts from the electromagnetic theory behind the measuring and visualization techniques.

2.1 Supersonic Jets, Shock Structure, Density Fluctuations, and Sound Production

2.1.1 Supersonic Jets and Shock Structure

When a stream of fluid comes out of a nozzle, and mixes with the surrounding nozzle, a jet is formed. The two dimensionless parameters that characterize these flows are the Reynolds Number $Re = vD/\nu$ and the Mach Number $M = v/c_s$, where v is the speed of the flow, D the exit diameter of the nozzle, ν the kinematic viscosity and c_s the local speed of sound. When M is close to or larger than 0.3, compressibility effects, that is density fluctuations, become important. The jet is supersonic for $M \geq 1$ at the exit.

Figure 1 shows the structure of a supersonic jet. The discontinuity at the edge of the nozzle produces a perturbation that propagates at the speed of sound. Each new perturbation catches on the previous one. The addition of these perturbations creates a conic region of very high density called shock. Starting with an expansion, a stationary pattern of shocks is formed in the supersonic region of the jet (Goldstein 1976).

As the speed decays the flow becomes subsonic and the shocks disappear.

2.1.2 Density Fluctuations

The equations that describe a compressible flow are more complicated than for the incompressible case. However, if small oscillations about a point of equilibrium are considered, the equations can be linearized. Monin and Yaglom (1987) have shown that if the equations of motion are written in terms of the vorticity Ω , the divergence D of the velocity, the entropy S , and the pressure P , all possible motions can be described by three non-interacting modes:

$$\begin{aligned}\frac{d\Omega(t)}{dt} &= 0 \\ \frac{dS(t)}{dt} &= 0 \\ \frac{d^2D(t)}{dt^2} + a_0^2k^2D(t) &= 0 \\ \frac{d^2P(t)}{dt^2} + a_0^2k^2P(t) &= 0.\end{aligned}\tag{1}$$

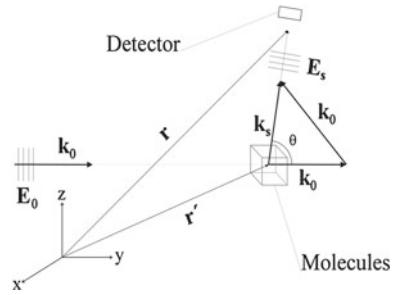
The incompressible vorticity (Ω) mode and the entropy (S) mode are stationary or move at constant speed. The acoustic (P) or potential (D) mode is related to pressure fluctuations that propagate at the speed of sound as can be seen from the wave equation. The entropic and acoustic modes, related to the compressible part of the flow, can be studied by Rayleigh scattering.

2.1.3 Acoustic Emission

There are several theories that try to explain acoustic emission by a jet based on the near field aerodynamics, either vortex interactions in the shear layer like pairing, tearing, or merging, or small scale motions due to instabilities generated at the nozzle. In general, it is now accepted that noise, in supersonic and subsonic jets, is made up of two basic components: one from the large turbulence structures and instability waves, the other from the fine-scale turbulence (Tam 1992, 1998, 2012; Veltin 2008). There are other possible sources of emission like the interaction of the flow with the shock waves and the feedback of acoustic waves that re-enter the flow.

Traditionally, experimental studies on acoustic waves are done by placing many microphones in the far field and correlating these measurements with events measured inside the flow. Most of the local techniques are intrusive, like hot wires or LDA and PIV that require homogeneous seeding (Goldstein 1983). Not only there is a problem trying to determine uniquely sources from far field measurements, but also certain phenomena like the diffraction of the acoustic waves by the mixing layer are usually not taken into account.

Fig. 2 Molecules scatter light in all directions. By selecting the orientation of the detector, we select the scattering angle and thus the size of the fluctuations to be studied



2.1.4 Rayleigh Scattering

The elastic scattering of an electromagnetic wave of wavelength λ_o by a neutral particle of dimensions smaller than the wavelength is known as Rayleigh scattering. In a static transparent gas, light is scattered homogeneously. If the gas is in motion or with strong density variations, the characteristics of the scattered light reflect the characteristics of the structure and motion of the gas (Jackson 1962). Figure 2 shows the wave vectors of the incident and scattered light.

The total scattered field can be obtained from the integral

$$\vec{E}_{ST} = \vec{E}_S(\vec{r}, t) \int d^3r' n(\vec{r}', t) \exp(-i\vec{k}_\Delta \cdot \vec{r}') = \vec{E}_S(\vec{r}, t) n(\vec{k}_\Delta, t), \quad (2)$$

where $\vec{E}_S(\vec{r}, t)$ is the field scattered by one molecule, $n(\vec{r}, t)$ is the distribution of molecules in the scattering volume V_s and $n(\vec{k}_\Delta, t)$ is the spatial Fourier transform of the density fluctuation. The scattered field has information about the motion of the molecules in the scattering volume through the spatial Fourier transform of the density.

2.2 Experimental Techniques

Rayleigh scattering has been used in two different ways: to visualize the flow and to obtain the spatial Fourier transform of the density fluctuations as a function of time. Shadowgraphs have been used also to visualize.

2.2.1 Visualization Methods; Rayleigh and Shadowgraphs

The shock structure can be visualized if the light scattered at small angles is captured with a lens and sent into a screen. The part of the laser beam that is not scattered is blocked (Azpeitia 2004) (see Fig. 3).

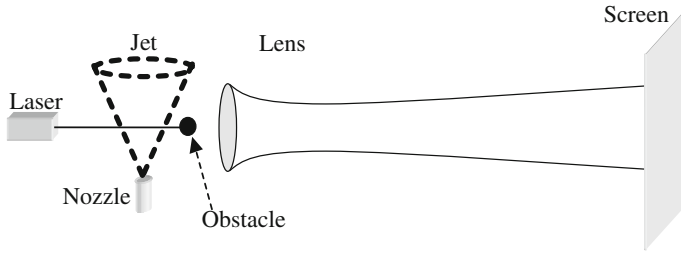


Fig. 3 Set-up for Rayleigh scattering

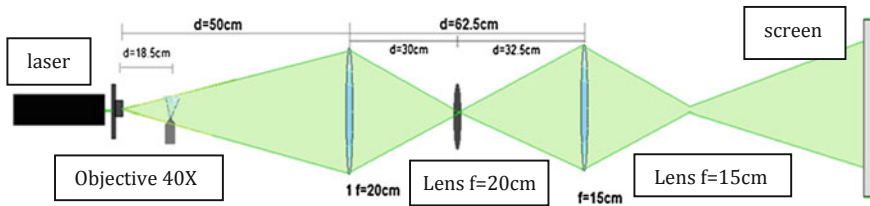


Fig. 4 Set-up for shadowgraphs (without attenuator in the middle) and Schlieren (with attenuator) (Salazar 2012)

If a cylindrical lens is placed in front of the laser, a sheet of light is formed and a larger section of the jet can be observed on the screen.

Shadowgraphs and Schlieren methods are used to detect changes in the index of refraction that cannot be seen by the naked eye (Settles 2001; Salazar 2012) (see Fig. 4).

2.2.2 Heterodyne Detection of Rayleigh Scattering

The amplitude of the light scattered by the molecules is extremely small, and it cannot be measured by a common diode. To solve this problem we mix it, on the surface of the photodetector, with a reference beam of light called the local oscillator. The local oscillator is displaced in frequency with respect to the incident beam by 110 MHz. This technique is known as heterodyne detection. Figure 5 shows the experimental set-up.

The beam that comes out of the laser is sent into an acoustic modulator. The modulator acts as a Bragg cell and several orders of diffraction come out. The order zero goes through without being deviated; we refer to this beam as incident or primary. The order one is diffracted at a certain angle, is less intense, and is displaced in frequency by 110 MHz. We will refer to this beam as the local oscillator. Both beams are manipulated so that they cross at an angle θ in the volume to be studied. The local oscillator is sent directly to a photodetector, the main beam is blocked just after the

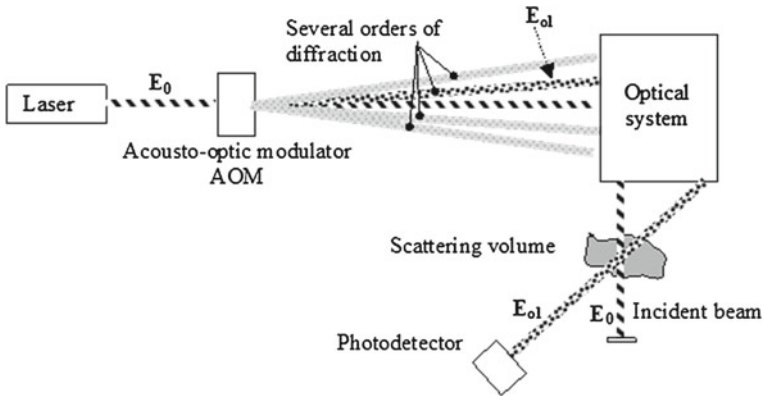


Fig. 5 The light from the laser is sent to an acousto-optic modulator to obtain several orders of diffraction displaced in frequency. One of these beams is used as the local oscillator to be mixed with the scattered light at the surface of the detector

scattering. On the photodetector then arrives the part of the incident field scattered at the angle θ and the local oscillator. The scattering angle determines the wavenumber of the fluctuations that are studied through the equation

$$k_{\Delta} = 2k_o \sin \frac{\theta}{2}, \tag{3}$$

where \vec{k}_o is the wavevector of the incident field, \vec{k}_{Δ} is the wavevector of the density fluctuations, $k_o = |\vec{k}_o|$, and $k_{\Delta} = |\vec{k}_{\Delta}|$.

The photodetector is sensitive to the intensity of the incident light, so the current it produces is proportional to the square of the electric field incident on its surface. The current of the photodiode is then proportional to

$$\left(\vec{E}_{ST} + \vec{E}_{OL}\right)^2 = \left|\vec{E}_{ST}\right|^2 + \left|\vec{E}_{OL}\right|^2 + 2\vec{E}_{ST} \cdot \vec{E}_{OL}. \tag{4}$$

The first two terms are constant and give a constant voltage. The first is too small to be extracted from the total value, and the second is of no interest. The third term gives a time dependent current that oscillates at the frequency difference of the frequencies of both electric fields, contains the information we are interested in, and is modulated by the amplitude of the local oscillator. The current proportional to this term is known as the heterodyne current (Yariv 1976).

It can be shown that the spectral density of the heterodyne current $I(\omega)$ produced by all the scatterers is of the form

$$I(\omega) = \frac{1}{8\pi k_0^2} \left(\frac{\eta e}{\hbar \omega_0} \right)^2 n_0 (r_0^R)^2 \frac{\varepsilon_0}{\mu_0} (\vec{E}_0 \cdot \vec{E}_D)^2 \int d^3k \left| W(\vec{k}_\Delta - \vec{k}) \right|^2 \left[S(\vec{k}, \omega - \omega_\Delta) + S(\vec{k}, \omega + \omega_\Delta) \right] \quad (5)$$

where η is the efficiency of the detector, n_0 the mean density, W is related to the Gaussian profiles of the beams and $S(\vec{k}, \omega)$ is the form factor defined by

$$S(\vec{k}_\Delta, \omega) = \frac{\left| n(\vec{k}_\Delta, \omega) \right|^2}{n_0 V} \quad (6)$$

Density fluctuations have been studied with Rayleigh scattering using other techniques (Panda and Seasholtz 1998).

3 Experimental Results

3.1 Visualization

When the near region is illuminated, the first shock created by the discontinuity at the nozzle can be observed (Fig. 6). The exiting flow expands as it comes out of the nozzle, but the stationary gas compresses it. The result is a high density region in form of a V.

When the flow is illuminated by a sheet of light, various shocks can be observed (Fig. 7).

In the shadowgraphs and Schlieren images the shock structure is better defined than in those shown above. Part of the internal structure can be observed. Figure 8 shows three first shocks for flows with different exit velocities. When the speed is very high, instead of a sharp cross, a flat region appears known as Mach's disk.

3.2 Heterodyne Detection and Spectral Densities

To obtain $I(\omega)$, the current that comes out of the photodetector $i(\omega, t)$ can be sent directly to a spectrum analyzer or acquired and processed with a computer. Due to the fact that the technique is sensitive to wave vector \vec{k}_Δ determined by the optical set-up, we can observe fluctuations propagating in different directions. To apply the previous equations, it is necessary to make sure that the beams remain Gaussian along the optical path. We have checked this in different points, and measured precisely the scattering volume.



Fig. 6 The flow goes upward. The first shock composed of an expansion and a compression is observed

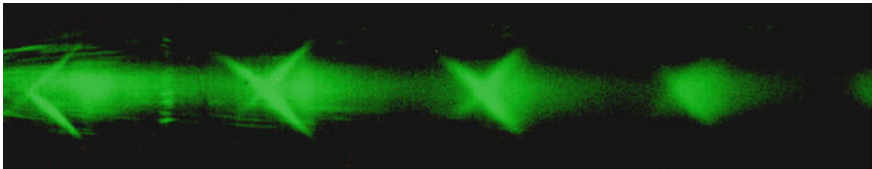


Fig. 7 The flow goes from left to right. A series of shocks can be observed

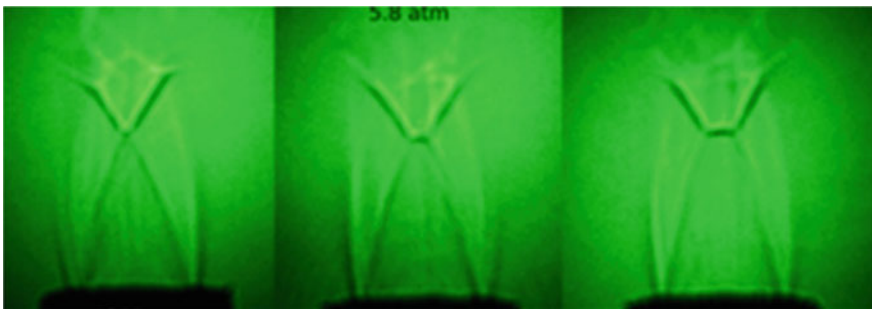


Fig. 8 First shock for three different exit velocities. The crossover from expansion to compression flattens as the speed of the flow increases

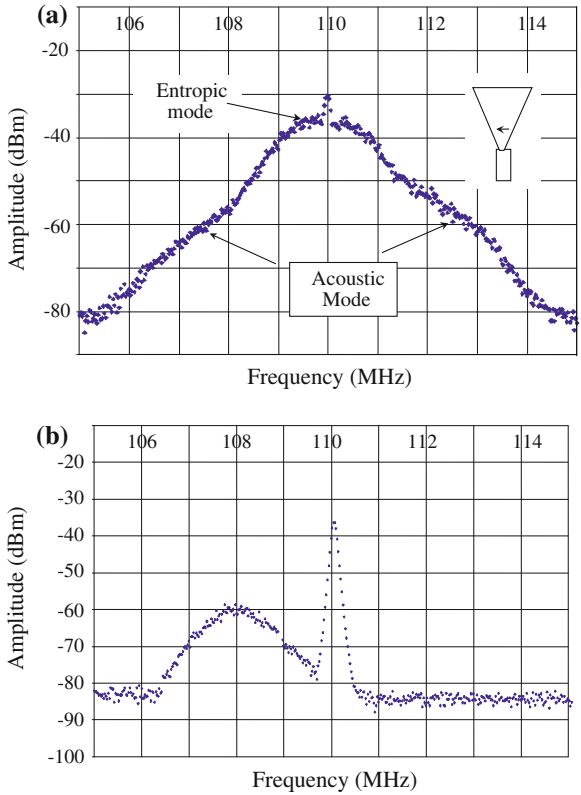


Fig. 9 Spectral densities for fluctuations traveling perpendicular to the flow. **a** centerline at 1.3 diameters from the nozzle, **b** outside the jet

We are also able to determine the width of the jet at each x location. When the flow exits the nozzle, the flow becomes narrower before it opens again; that is, even though it comes out of a contraction, it behaves as if it went through a contracting divergent nozzle (Carreño Rodríguez 2010).

Figure 9a shows a spectral density obtained with a spectrum analyzer for density fluctuations in the axis of the jet, at 1.3 diameters from the nozzle, propagating in a direction perpendicular to the flow. The spectrum is symmetric centered at the frequency of the optical modulator. The spectrum appears to be broad and corresponds mainly to fluctuations of entropic origin due to the turbulent nature of the flow. However, a small bump on either side of the center, at a frequency that can be identified with an acoustic fluctuation can be observed.

Figure 9b shows density fluctuations outside the flow. The center of the peak corresponds to an acoustic wave traveling in a direction opposite to the wave vector defined by the optics.

Figure 10a shows the spectral density obtained at the same point than Fig. 9a but for fluctuations traveling parallel to the flow. In this case, the fluctuations are convected with the flow and the entropic peak is displaced to the right because of the Doppler shift. The local mean velocity can be measured from the frequency shift. In this figure the acoustic peak cannot be observed on the right, probably because it is submerged under the entropic peak. The peak on the left comes from outside of the jet due to the length of the scattering volume.

Figure 10b is similar to Fig. 10a but at a different location along the centerline. It is important to notice a low frequency peak.

From Fig. 10 two important observations can be made. First, if the acoustic peak exists, it could be hidden under the broad entropic peak; or its frequency could be so close to the entropic frequency that they form together a broad peak and the two frequencies cannot be identified separately. The second observation is that in certain locations, always at the centerline of the jet, a peak appears at a much lower frequency than the entropic peak.

3.3 Signal Processing and Parametric Periodgrams

From the conclusions above, it became necessary to search for an appropriate signal processing that would increase the spectral resolution. The first thing to be considered, besides Nyquist theorem, is that a very high sampling frequency would indeed give a very faithful reconstruction of the signal in time but extremely poor in the frequency domain. The spectral densities obtained with the spectrum analyzer showed the need for much better frequency resolution. The second thing is the method to obtain a spectral density with less noise.

This seems a simple matter but most oscilloscopes and spectrum analyzers do not allow the user to choose freely the sampling frequency.

After analyzing several techniques, we decided to use Burg parametric periodgrams. If the acquisition is done right, there is a wide range within which the spectral density is independent of the number of parameters (Alvarado Reyes 2004, 2010).

3.4 Slow Mode and Shock Structure

Figure 11 shows a series of spectra for fluctuations traveling perpendicular to the flow, obtained with periodgrams at different locations along the centerline.

Three peaks are visible. The acoustic peak is always at the same location. The entropic peak changes with the local speed of the flow. As expected, the speed of the flow changes very little in the supersonic region. The slow peak appears and disappears along the centerline and changes slightly its frequency. It is interesting to note that when the new peak has its highest amplitude, the acoustic peak disappears and vice versa. We are searching for an explanation for this effect.

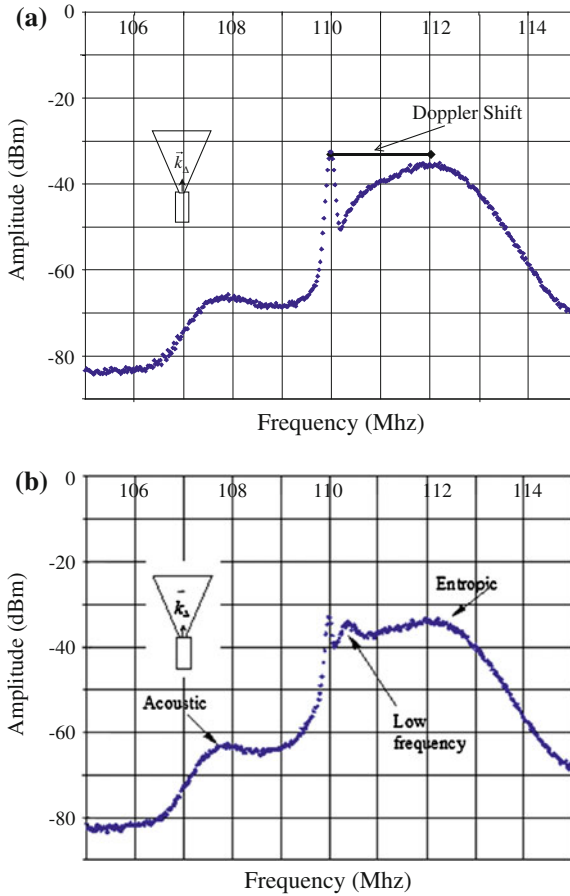


Fig. 10 Spectral densities for fluctuations traveling parallel to the flow. **a** at 1.3 diameters from the nozzle, **b** at another location along the centerline. A low frequency peak appears at certain positions. The acoustic peak on the left comes from outside of the jet. For small angles the scattering volume is very long in the direction perpendicular to the wave vector

If we compare Figs. 7 and 11, we obtain Fig. 12 where we can determine that the regions of maximum amplitude of the low frequency peak, correspond to the crossover between expansion and compression in the shocks. The x coordinate (along the centerline of the jet) is given in multiples of the nozzle diameter.

This low frequency can be related to the interaction between the shock structure and the flow. The shock structure appears very stable in all the images. However, there is a possibility that it oscillates at a frequency that cannot be detected by the eye. This will be determined with further tests with a high speed camera. In both cases, this slow mode would be maximum close to the shock structure.

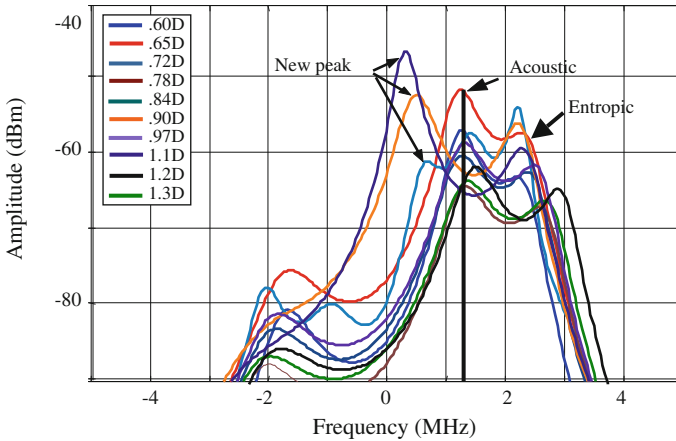


Fig. 11 Spectral densities obtained with Burg’s parametric periodgrams at various positions along the centerline of the jet

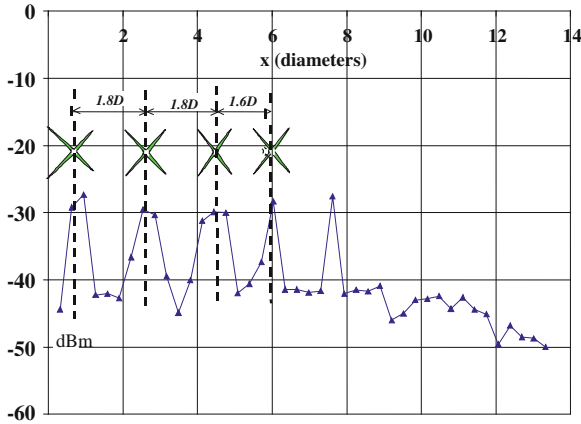


Fig. 12 Comparison between the locations at which the low frequency peak is maximum and the shock position along the centerline

3.5 Emission Pattern

We have taken data at many positions inside and outside the jet, and processed the signals with Burg’s periodgrams, for different directions of the wave vector. At each point, we determined the direction for which the amplitude of the acoustic fluctuation is the largest. Figure 13 shows the spectra at the same point for different directions of the wave vector.

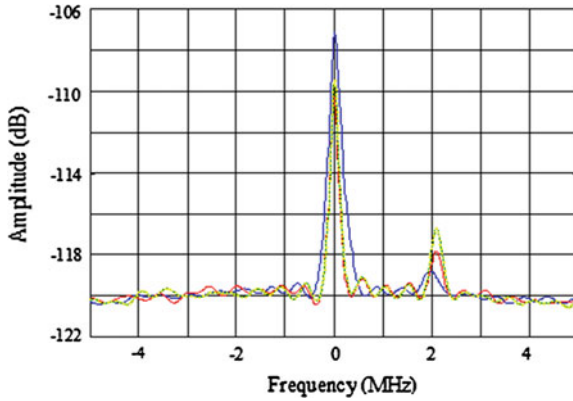


Fig. 13 Periodgrams obtained at the same point for different directions of the wave vector outside the jet. The maximum amplitude corresponds to the direction of propagation of the fluctuation

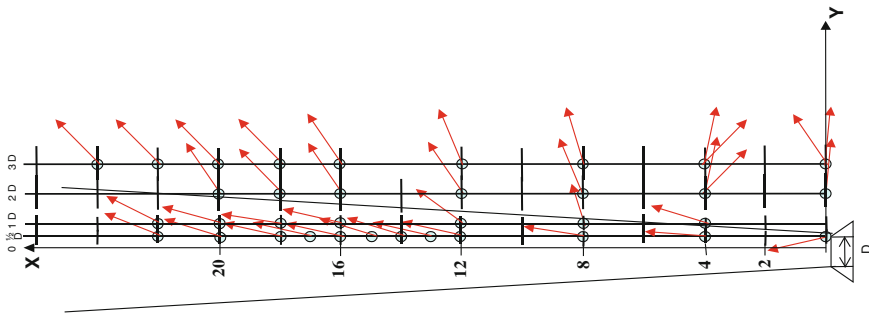


Fig. 14 Acoustic radiation pattern for a supersonic jet

We define the direction of maximum amplitude as the direction of propagation of the acoustic fluctuations. As shown in Fig. 14, we were able to construct an acoustic emission pattern for a jet.

It must be pointed out that with our technique, we can only detect ultrasound waves. To reduce the frequencies we can detect for acoustic waves a larger wavelength for the incident laser is required.

3.6 Particle Image Velocimetry (PIV)

So far, we have been able to determine the speed of the flow either by the Doppler shift of the spectrum, or by the angle of the shock wave. The two measurements give different results, probably due to the lack of precision in the measurement of the angle. To have a better measurement to compare with, we are in the process of

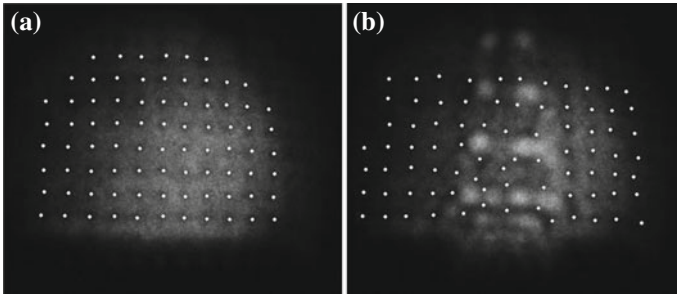


Fig. 15 Variation of the index of refraction. **a** Original dot net, **b** dot net modified by the jet flow

doing Particle Image Velocimetry on the flow. It is very difficult to seed high speed gas flows because most commercial particles are too heavy to follow the flow. The way seeds are introduced must not affect the flow speed and the distribution should be homogeneous at least for some time. It is well known that turbulence and large vertical motions redistribute the particles (Echeverría Arjonilla 2013).

In our experiments, we have detected that the seeds modify the shock structure. The first shock occurs closer to the nozzle, the angle becomes larger, and thus the local speed decreases. We are not sure yet whether it is the presence of the titanium dioxide particles or the system of injection that produces this modification.

3.7 *Quantification of the Index of Refraction*

The images shown in Figs. 6, 7, and 8 have been used so far to provide only qualitative information, except for the determination of the angle of the shock wave and thus the local speed.

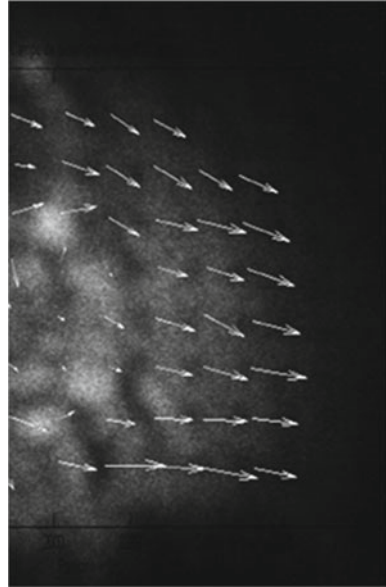
Schlieren images and shadowgraphs can be used, with the help of a net of dots, to quantify the variation of the index of refraction. To do so, an image of a net of points is placed behind the location where the flow will be. An image without flow is taken as shown in Fig. 15a and b (Porta 2013)

The change in the position of each dot is related to the change in the index of refraction and thus to the density. Figure 16 shows the field of displacements of the dots. We are on the process of relating this field with the size of the shocks.

4 Conclusions and Future Work

Rayleigh scattering has proven to be a very useful tool because it is non-intrusive, does not require seeding, and measures directly the motion of the fluid.

Fig. 16 Displacement field which is proportional to the gradient of the index of refraction



Heterodyne detection of Rayleigh scattering can differentiate among three different density fluctuations: acoustic waves propagating at the speed of sound, entropy fluctuations convected by the flow velocity, and a low speed fluctuation that might be related to interaction between the flow and the shock structure. It is still necessary to determine if the shock structures fluctuate with time.

With this technique we have observed that, contrary to what most textbooks prove, a contraction can produce a supersonic flow and a stable shock structure. We have shown that the flow gets narrower just outside of the nozzle and then reopens again (Carreño Rodríguez 2010). This happens in a length shorter than a diameter.

This technique can also be used to measure the local speed of flow in any direction. The precise measurement of the frequency, that can be done when the spectral density is calculated with periodgrams, gives a precise measurement of the speed.

The system is sensitive to the direction of propagation of the fluctuations, so it can be used to determine the acoustic radiation pattern of the flow for a wave number determined by the optics. It is quite easy to change the scattering angle, and thus the wave number. Its limitation consists that only fluctuations with the wave vector determined by the optical set up can be detected.

The spectral density is related to the energy, so it can be seen how the energy is distributed among the different kinds of fluctuations for each wave number.

The supersonic structure can be visualized with Rayleigh scattering, with Schlieren images and with shadowgraphs. Each technique gives different information about the shock structure and about the changes in the index of refraction.

The work that is presently being done in PIV and the quantification of the index of refraction will complement the information we already have. The visualization of

the flow simultaneously to the shock structure is still a big challenge, because the shocks scatter an enormous amount of light that hides all other motions.

The biggest problem of the heterodyne detection of Rayleigh scattering is the spatial resolution of the scattering volume. The scattering volume is formed by the intersection of the local oscillator and the primary beam. Very small angles (about 2 mrad) have to be used to detect lower frequencies of acoustic interest. As a consequence, the scattering volume is very thin but very long, so the spatial resolution in the direction perpendicular to the direction of propagation is very bad. Presently, a system with two local oscillators crossing the primary beam at the same angle in the same location is being developed. Correlations between the two signals should help reduce the problem.

In textbooks, shocks are lines representing sudden changes in the density. We know however, that the change in density is continuous. Our next interest is to determine experimentally the changes in the density across the shocks, and give an operational way to measure the interface. Also Schlieren images and shadowgraphs will show if there is any internal structure.

Acknowledgments We acknowledge support from UNAM through DGAPA projects IN107599, IN104102, IN116206 and IN117712. Also the participation of several undergraduate students: Cesar Aguilar, Carlos Azpeitia, Alejandro Carreño, Yadira Salazar, Carlos Echeverría, and David Porta.

References

- Aguilar C (2003) Detection of acoustic waves in a supersonic jet using Rayleigh scattering. BS thesis, Department of Physics, School of Science, UNAM, Mexico City, Mexico
- Alvarado Reyes JM (2004) Spectral analysis of signals from Rayleigh scattering experiment. M.E. Thesis, School of Engineering, UNAM, Mexico City, Mexico
- Alvarado Reyes JM (2010) Técnicas modernas para el tratamiento de señales turbulentas, PhD thesis, Universidad Nacional Autónoma de México
- Azpeitia C (2004) Use of Rayleigh scattering to localize acoustic sources in a supersonic jet. BS thesis, Department of Physics, School of Science, UNAM, Mexico City, Mexico
- Bodony DJ, Lele SK (2006) Low frequency sound sources in high-speed turbulent jets. Annual Research Briefs, Center for Turbulence Research, Stanford University, Palo Alto. Ca, USA
- Carreño Rodríguez AS (2010) Reconstruction of gaussian beams to increase the spatial resolution in a Rayleigh scattering experiment. BS thesis, Department of Physics, School of Science, UNAM, Mexico City, Mexico
- Chapman CJ (2000) High speed flow. Cambridge University Press, Cambridge
- Echeverría Arjonilla C (2013) PIV measurements in a supersonic flow. BS Thesis, Department of Physics, School of Science, UNAM, Mexico City, Mexico
- Goldstein ME (1976) Aeroacoustics, 1st edn. McGraw-Hill, USA
- Goldstein RJ (1983) Fluid Mechanics Measurements, 1st edn. Edit, Hemisphere, USA
- Jackson JD (1962) Classical electrodynamics. John Wiley & Sons Ltd, New York
- Monin AS, Yaglom AM (1987) Statistical fluid mechanics. MIT Press, Cambridge
- Nichols JW, Ham FE, Lele SK, Monin P, Ham FE, Lele SK, Moin P (2011) Prediction of supersonic jet noise from complex nozzles. Annual Research Briefs, Center for Turbulence Research, Stanford University, Palo Alto. Ca, USA

- Panda J, Seasholtz R (1998) Density measurement in underexpanded supersonic jets using Rayleigh scattering. 36th AIAA Aerospace Sciences Meeting and Exhibit, 1998, [10.2514/6.1998-281](#)
- Porta D (2013) Interfaces in a supersonic jet using shadowgraphs. BS Thesis, Department of Physics, School of Science, UNAM, Mexico City, Mexico
- Salazar Romero MY (2011) Advanced optical techniques applied to fluid dynamics. BS Thesis, Department of Physics, School of Science, UNAM, Mexico City, Mexico
- Settles GS (2001) Schlieren and shadowgraph techniques. Visualizing Phenomena in Transparent Media, Edit, Springer, USA
- Stern C, Grésillon D (1983) Fluctuations de Densité dans la Turbulence d'un Jet. Observation par Diffusion Rayleigh et Détection Hétérodyne. *J Phys* 44:1325–1335
- Tam C (2012) Computational aeroacoustics: A wave number approach. Cambridge University Press, Cambridge
- Tam C (1998) Jet Noise: Since 1952. In: Theoretical and computational fluid dynamics. Springer, New York
- Tam C (1992) Broadband shock associated noise from supersonic jets measured by a ground observer. 30th Aerospace Sciences Meeting and Exhibit, 1992, [10.2514/6.1992-502](#)
- Veltin J (2008) On the characterization of noise sources in supersonic shock containing jets. PhD Thesis, Pennsylvania State University, Google Books
- Yariv A (1976) Introduction to optical electronics. Holt, Rinehart and Winston, New York